Contents

1 General context

1.1 Neutrino physics

1.1.1 A brief history of the neutrino

The existence of neutrinos was first postulated by W. Pauli in 1930 to explain the continuous energy distribution of the β-decay while preserving energy conservation. It needed to be a neutral, light-weighted fermion, hence the name neutrino (the little neutral in Italian). After its first observation (an electron antineutrino) by the Savannah experiment in 1956, multiple experiements in the second half the 20th century led to a good understanding of the particle while being theoritically described accordingly by the Standard Model (SM) of particle physics. In the SM, the neutrino is a massless, left-handed (antineutrino is right-handed), neutral lepton coming in three flavors: electronic ν_e, muonic ν_μ and tauic ν_τ. It interacts through weak interaction only and has a very small cross section of $\sim 10^{-38}\,\mathrm{cm}^2$ at 1 GeV, making it really tricky to detect.

However this picture has its imperfections, in 1970 the Homestake experiment detected only 40 % of the predicted electron neutrinos in the solar neutrino flux. The Super Kamiokande Neutrino Detection Experiment in 1998 and the Sudbury Neutrino Observatory in 2002 [5] confirmed this discrepancy and established the existence of a new physical phenomenon theorized by B. Pontecorvo in 1967: neutrino flavor oscillations. The capacity for neutrino to oscillate between flavors during propagation goes beyond the standard model the SM for at least two reasons: it violates total lepton number conservation and it requires non-zero neutrino masses.

The number of neutrino masses is not fully established, a forth (or more) neutrino mass eigenstate could exist in the form of a sterile neutrino(s). In the following, only three neutrino masses (m_1, m_2, m_3) are considered. An upper bond of around 1 eV have been established, and constraints on the mass differences $\Delta m^2_{ij} \equiv m_i^2 - m_j^2$ could be set. As of today, two of theme have been measured, leaving two possible mass hierarchy: normal order (NO) $(m_3 \gg m_2 > m_1)$ and inverted order (IO) $(m_2 > m_1 \gg m_3)$.

The mass of the neutrino is descirbed through what is known as a seesaw mechanism in beyond SM formulations and two formulations of the nature of the neutrino are in competition. The Dirac formulation consists of adding two degrees of freedom in the form of a right-handed sterile neutrino and preserves the lepton numbers conservation. The Majorana formulation postulate that neutrinos and antineutrinos could oscillate between one another and thus that lepton numbers are not conserved quantities. The neutrino is the only known neutral elementary particle and for this reason it is the only particle which could be of Majorana nature. This is currently tested by searching for a neutrinoless double β-decay ($0\nu2\beta$) which would effectively violate the electronic lepton number [2].

1.1.2 Flavor oscillations

Neutrino oscillations are described by a difference between the mass eigenstates $(i = 1, 2, 3)$ at work during propagation, and the flavor eigenstates $(\alpha = e, \mu, \tau)$ at work at the interactions. The unitary transformation relating the two eigenstate states is written as the unitary Pontecorvo-Maki-Nakagawa-Sakata (PMNS) mixing matrix U. The PMNS matrix can be parameterized by three mixing angles: θ_{12}, θ_{23}, θ_{13} as well as one Dirac phase: δ and two Majorana phases: α_1, α_2. Three additional non-physical phases can be absorbed in the lepton fields and the two Majorana phases do not affect oscillations and are thus ignored in the following [5]. We can then write the realtion between the two sets of eigenstates as:

$$|\nu_\alpha\rangle = \sum_i U^*_{\alpha i}|\nu_i\rangle \quad \text{with} \quad U = \begin{pmatrix} 1 & 0 & 0 \\ 0 & c_{23} & s_{23} \\ 0 & -s_{23} & c_{23} \end{pmatrix} \begin{pmatrix} c_{13} & 0 & s_{13}e^{-\mathrm{i}\delta} \\ 0 & 1 & 0 \\ -s_{13}e^{\mathrm{i}\delta} & 0 & c_{13} \end{pmatrix} \begin{pmatrix} c_{12} & s_{12} & 0 \\ -s_{12} & c_{12} & 0 \\ 0 & 0 & 1 \end{pmatrix}$$

where the PMNS matrix has been explicitly written as a product of three rotation matrix and using the convention: $c_{ij} \equiv \cos\theta_{ij}$ and $s_{ij} \equiv \sin\theta_{ij}$. One can now compute the propability for muon neutrinos of energy $E \simeq p$ to oscillate to an electron neutrino over a distance $L \simeq t$ in vacuum (working in natural units: $\hbar = c = 1$). Using a quantum mechanical framework, it suffices to express the neutrino states in term of the mass states which are Hamiltonian eigenstates by definition:

$$|\nu(t=0)\rangle \equiv |\nu_\mu\rangle = \sum_i U^*_{\mu i}|\nu_i\rangle \quad \text{and} \quad |\nu(t)\rangle = \sum_i U^*_{\mu i} e^{-\mathrm{i}E_i t}|\nu_i\rangle$$

Where the energy E_i can be written as: $E_i \equiv \sqrt{p^2 + m_i^2} \simeq p + \frac{m_i^2}{2p} = E + \frac{m_i^2}{2p}$. The propability of oscillations over L is as follows:

$$P(\nu_\mu \to \nu_e, L) = |\langle \nu_e | \nu(t) \rangle|^2 = \left| \sum_i U_{ei} U_{\mu i}^* \exp\left(-\mathrm{i} \frac{m_i^2 L}{2E} \right) \right|^2$$

After some computation, the final result at second order in small quantities $\sin\theta_{13}$ and $\sin(\Delta m_{21}^2 L/4E)$ is :

$$P(\nu_\mu \to \nu_e, L) = \alpha \sin^2\left(\frac{\Delta m_{31}^2 L}{4E}\right) + \beta \sin^2\left(\frac{\Delta m_{21}^2 L}{4E}\right) + \gamma \sin\left(\frac{\Delta m_{21}^2 L}{4E}\right) \sin\left(\frac{\Delta m_{31}^2 L}{4E}\right) \left(\frac{1}{2}\cos\delta - \sin\delta\right)$$

where α, β, γ are functions of θ_{12}, θ_{23}, θ_{13} only [5]. From this formula, two pieces of information will be of importance in this manuscript. Firstly, oscillation probability peaks and vanishes as a function of L/E, and secondly, oscillation experiements give information on the mass differences Δm_{ij}^2 and the angles θ_{ij} but cannot access absolute mass values.

On another hand, this paradigm allows to quantify charge conjugation and parity (CP) violation in neutrino oscillations by looking at the difference $P(\nu_\alpha \to \nu_\beta) - P(\bar{\nu}_\alpha \to \bar{\nu}_\beta)$. It can be shown that this difference is proportional to the sinus of the Dirac phase δ (when $\alpha \neq \beta$) [5]. It is thus commonly referred as the CP violation phase δ_{CP} as a zero value would imply CP conservation. Its value is yet fully unknown.

When neutrinos travel through matter we have to take into account an additional potential coming from the charged current interaction of ν_e with electrons inside matter. Those interactions are absent from the muonic and tauic sectors as muons and tauons don't appear in regular matter. Moreover, neutral current interactions are equivalent for all three flavors and do not impact the oscillation mechanism. Propagation in constant-density matter will have an effect of resonant effect of oscillations depending on density and will either enhance neutrino or antineutrino oscillations between two flavors at resonance depending on the sign of Δm^2. This property can thus give us access to the sign of Δm_{31}^2 and to the mass hierarchy [5].

1.2 The Deep Underground Neutrino Experiment

The Deep Underground Neutrino Experiment (DUNE) is an international collaboration involving more than 1400 collaborators from over 200 institutions in over 30 countries. Its main purpose is the study of neutrino flavor oscillations in an underground beam over a long distance.

1.2.1 Physics program

High-precision measurement of the various parameters involved in neutrino flavor oscillations could determine the sign of Δm_{31}^2 effectively fixing the mass ordering, the octant of θ_{23} which is not avalaible at first order, in addition to lower incertitudes on already measured quantities.

Comparing neutrino and antineutrino oscillations and measuring δ_{CP} with high-precision would allow investigations of CP violation in the lepton sector. This could shed light on baryogenesis in the early univers as CP violation is one of the three Sakharov conditions that must be satisfied by a process generating matter and antimatter at different rates.

The detection of galactic core collapse supernova neutrino bursts requires good sensitivity in MeV-energy and a good understanding of the energy and time signature of such a signal. Neutrino being the first messengers to reach Earth in a supernova, DUNE will be part of the SuperNova Early Warning System (SNEWS) and set off an early alert of a galactic supernova event for observatories minutes to hours before the supernova electromagnetic signal reaches Earth. This network would allow to measure the first seconds of the supernova electromagnetic signal which contains information about what occurred in the core of the star [6].

Searching for an hypothetical proton decay $p \to K^+ \bar{\nu}$ requires identifying the short kaon tracks in the background induced by cosmic muons, and a good time resolution

1.2.2 Installation

The DUNE final installation is located in the United States of America and composed of a muon neutrino beam, a near detector at the Fermi National Accelerator Laboratory (Fermilab) near Batavia, Illinois, and a far detector at the Sanford Underground Research Facility (SURF) in Lead, South Dakota (cf. Figure 1).

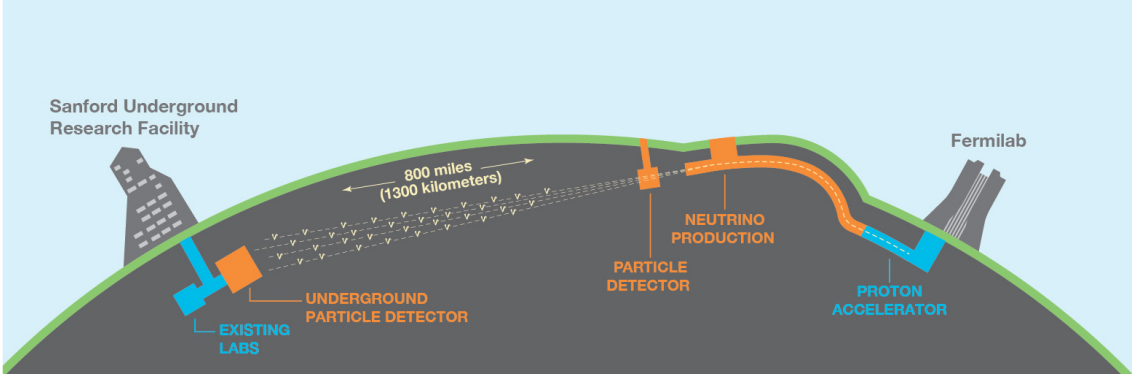

Figure 1: DUNE installation. From left to right: the far detector at SURF, the near detector and the proton accelerator at Fermilab

The Fermilab 1.2 MW main injector produces a 120 GeV proton beam hitting a large target producing a shower of hadrons (mostly pions) then focused by three 300 kA magnetic horns into a 200 m long decay pipe. 99.9 % of the charged pions will decay into muons and muon neutrinos which will then travel to the near detector 400 m downstream. The horns current polarity can be swapped to select only positive or negative pions (with 10 % contamination) leading in a muon neutrino or muon antineutrino beam respsectively. This will allow seperate measurement of neutrino and antineutrino oscillation which is crucial to the determination of δ_{CP}. An additional 1 % contamination of electron neutrinos from kaons and muon decays is expected.

The near detector aims to measure the beam parameters before any neutrino flavor oscillation in the beam allowing to isolate the effect of oscillations. It will be composed of several modules and their will be gazeous and/or liquid argon detectors. The far detector is located 1285 km downstream of the beam and 1480 m underground in a former gold mine. It is composed of four liquid argon time-projection chambers (LArTPC) for a total of 40 kt of fiducial volume. Having the same target in the near and far detectors effictively reduces systematic errors, especially on the difference of value of the neutrino cross section, which is moreover not well known in argon.

1.3 The DUNE group at IJCLab

This intership is carried out at the Irène Joliot-Curie laboratory (IJCLab) in Orsay, France, from the National Institut of Nuclear Physics and Particle Physics (IN2P3) from the French National Center for Scientific Research (CNRS). The group working on the DUNE project is composed of three permanant researchers: Thibaut Houdy, Yoann Kermaïdic and Fabien Cavalier and two Ph.D. students: Emile Lavant and Matteo Bedes

The group at IJCLab is specialized in the vertical drift technology and is in charge of the design and production of the chemineys hosting the electronic devices responsible for the outgoing data at the top of the vertical drift detectors, as well as the printed circuit board (PCB) interface between the LAr and the outside. The group is also developing modules for data analysis at low energies in ^{39}Ar [...]

Under the direction of Dr. Houdy, this intership aims at developping the analysis of Michel electrons in the prototype detector for low-energies calibration of LArTPCs alongside other collaborators: Matteo Galli at the Astroparticle and Cosmology (APC) laboratory in Paris, France, and Laura Pérez Molina at the Centre for Energy, Environmental and Technological Research (CIEMAT) in Madrid, Spain.

2

2.1 The ProtoDUNE experiements

Various LArTPC prototypes (ProtoDUNE) for the DUNE far detector are being built and operated at the neutrino platform of the European Organization for Nuclear Research (CERN). Two different geometries, namely vertical drift (VD) and horizontal drift (HD), will be used in the LArTPCs of DUNE and are tested at CERN. The differences is on the direction of the applied electric field lines and of the drifting electrons which are the main source of information in the detectors.

The first prototype, ProtoDUNE-SP for single phase, operated between 2018 and 2020.

Complementarity, Advantages: is it good if the particle crosses the detection planes? why?

VD data at the end of 2024

2.2 Vertical drift TPC

The DUNE vertical drift far detector is 17.8 m width, 65.8 m depth and 18.9 m height TPC. It consists in a large volume of LAr, acting as a calorimeter and a scintillator, contained in a cryostat at $-184\,°\mathrm{C}$. Inside the volume are two anodes at the top and bottom of the TPC and a cathode suspended halfway up, creating two 6.5 m vertical drift volumes. The cathode is set at $-294\,\mathrm{kV}$ while the anodes, in direct contact with the entire cryostat, are set to the ground. The electrons ionized by the charged particles will drift up in the upper volume and down in the lower volume under the influence of the $450\,\mathrm{V/cm}$ electric field. The active volume is surrounded by a field cage which ensures the homogeneity of the field lines inside the volume. By convention the drifting axis is the x-axis and the beam axis is the z-axis.

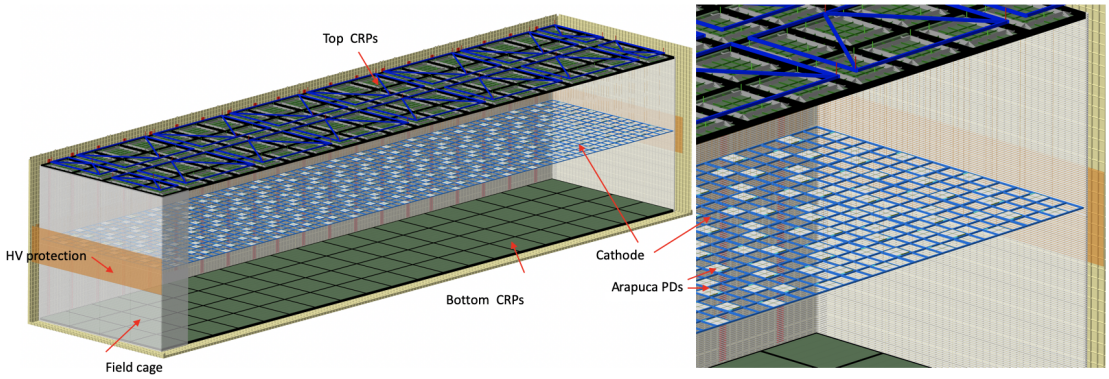

Figure 2

The cathode is divided in chuncks intependantly suspended to minimize deformation of the superstructure from which it hangs Each chunk is tiled with evenly distributed photon detectors (PD) in some of the square holes. The LAr can freely move from top to bottom of the TPC maximazing the total active volume.

The anodes are each composed of three charge-readout planes (CRP) immersed in the LAr. Multiple holes allow the drifting electrons to pass through each layer while evenly spaced stripes and their surfaces are used to tag their passage. The first two layers, U and V, are induction planes set at $-340\,\mathrm{V}$ and $0\,\mathrm{V}$ respsectivley. They stripes form an angle of $-35°$ and $+35°$ with the stripes of the collection plane respsectivley. Charged particles passing through the induction planes are tagged by the bipolar (zero integral) signal in the nearest stripe. The outermost layer, W, is a collection plane set at $+900\,\mathrm{kV}$ which will collect the drifting electrons resulting in a unipolar (positive integral) signal. The conjugation of the induction plane signals allow the reconstruction of the position of the energy deposit in the yz-plane while the collection plane has the best signal-to-noise performance and charge resolution and is thuse used to reconstruct the electron energy [3].

A photon detection system is used to tag an initial time point at the reception of the scintillation photon. The collected electron being thermalized, their drift speed is determined by the applied electric field. The

elapsed time between photon and electron reception allow to reconstruct the x-position of the energy deposit by the charged particle.

2.3 Liquid argon

A charged particle through-going LAr deposit energy *via* ionizing the Ar atoms and *via* excitation [3]. The ionization energy of the Ar being 20 eV, a typical cosmic muon with a $\mathrm{d}E/\mathrm{d}x$ of 2 MeV/cm would ionize up to 200,000 electrons per centimeter. The ionized argon atoms Ar^+ will form molecular bond Ar_2^+ with neutral Ar atoms before recombining with surrounding free electrons to excimers Ar_2^*. In absence of exterior electric field, the charged particle will most likely only excite Ar atoms creating Ar_2^* without free ionized electrons. Higher the electric field, More easily the Ar atoms will be ionized. The excimers will return to the fundamental state 2Ar by dissociating and emitting scintillation UV photons of 128 nm of wavelength.

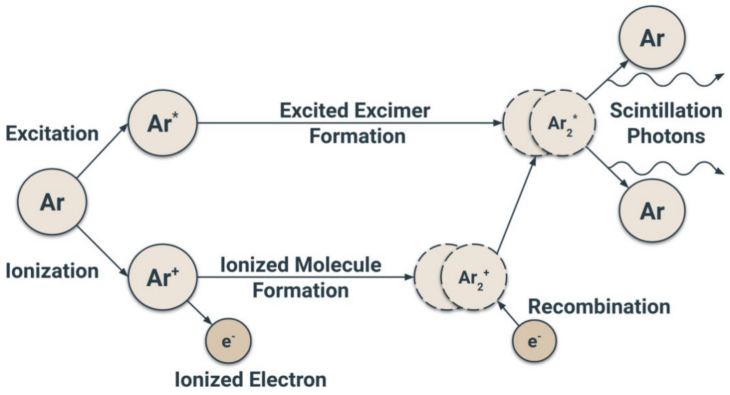

Figure 3: **[ref?]**

As the inonization electrons propagate in LAr, they will inonize more Ar atoms and also deposit their energy via radiative losses, namely bremsstrahlung radations, that are present at all electron energies leading to electromagnetic showers of secondary photons and electrons. The bremsstrahlung photons will be reabsorbed by the medium. They may inonize electrons through the photoelectric effect, Compton scatter or annihilate in electron-positron pairs [3]. The scintillation photons can propagate freely in the LAr as it is transparant at this frequency in absence of impurity. This also mean that the mean free path of scintillation photons can be a measure of the liquid purity.

Dopping LAr with Xe is studied as it would act as a wavelength shifter by absorbing the scintillation photons and reemit more longer-wavelength photons. This has the advantages of increasing the light yield and the distance traveld by scintillation photons as the wavelength-shifted photons are less subject to impurities.

2.4 LArSoft

The liquid argon software (LArSoft) is a set of programs using the ROOT library and is used for all the steps of data analysis important to DUNE, from simulation to track reconstruction. The different outputs of steps of execution of LArSoft are the base data for the data analysis modules.

The first step is generating incoming particles and their initial parameters: energy, momentum (direction)and position. The Cosmic Ray Simulationfor Kaskade (CORSIKA) program provides extensive simulation for air showers initiated by high energy cosmic ray particles.

The next step consists in simulating particle propagation through LAr, computing their energy deposits and trajectories. Then, the following ionizations, scintillations, as well as electromagnetic showers and light matter interaction are performed. Those two steps are both handled by the Geometry And Tracking (Geant4) program using Monte Carlo methods.

Once the interactions with the medium is computed, the Wire-Cell Toolkit (WTC) simulate the detector response. At this stage the simulated data should be similar to what is expected to come out of the data acquisition systems (DAQ) (after a necessary stage of data conversion) in real-world experiemntal situation.

This final step is crucial as it is common to simulated and experiemental data and will be used to analysis in the final installation of DUNE. The reconstruction stage build three-dimensional particle tracks from the detector outputs. From the raw ADC counts of the induction and collection wires, the program extract the physical signal of passing electrons by removing the static noise, decovolving the electronic response and defining a region of interest (ROI) to discriminate relevant signals from unusable ones. Then a hit is reconstructed, that is a coincidence between gaussian bumps fit the previously reconstructed signals on the wires of each three planes. A hit is then associated to a 3D space point as well as an associated deposited energy in the LAr. Recognition algorithms such as Pandora or TrajCluster are then used to reconstruct clusters of hits produced by the same particle. From this information can be derived track-like clusters, shower-like clusters and calorimetric measurements.

The development of a typical module will involve the full simulation of an event of interest using LArSoft and its analysis first using the true simulated data then gradually replace it by reconstructed data. The comparison of reconstructed data and true simulated data for the same event is useful to spot inconsistencies in the process of development and to charcterize the strength and shortcomings of the module.

3 Michel electron track reconstruction

3.1 Michel electrons

In the main muon decay channel $\mu^{\pm} \to e^{\pm}\nu_{\mu}\nu_{e}$ (ν and $\bar{\nu}$ undistinguished), the electron (or positron) is called a Michel electron. all antimuons decay to Michel positrons but only about a quarter of all muons decay to Michel electrons, the three quarters left being captured by argon atoms. During its propagation the muons will inonize electrons, some of which will be high-energy enough to travel a significant distance and produce their own track. Those electrons are known as Δ-rays and should not be confused with Michel electrons.

Michel electrons are theoritically well-known and their energy is continuously distributed between 1 to 50 MeV, making them a good candidate for low energy calibration of the LArTPCs. A good xunderstanding of the detector response to low energy electrons signal is decisive in the detection of supernova signals for SNEWS or in the understanding of electromagnetic showers in the detector. Preliminar tests have been and will be carried out at CERN on the ProtoDUNEs using comic muons as a source of Michel electrons.

3.2 Track reconstruction

This study lies heavily on a first attempt at Michel electron track reconstruction in the ProtoDUNE-SP by A. Rafique *et al.* [3]. When considering the reconstruction of Michel electron events the first step is a thorough selection of the muon and candidate Michel electron events to keep only the events with the best reconstruction. As cosmic muons won't be rare **how many?** there is no need to be afraid a dumping many events. Once kept only the muon believed to decay in Michel electrons, the selection on Michel electrons hit is characterized on simulated data with two parameters. The purity is the fraction of reconstructed Michel electron hit that are from actual Michel electron and the completness is the fraction of true Michel electron hit that are selected.

Using simulation, the cone opening angle θ is optimized at $60°$ **how?** *and the cone length d is* 20 cm *in order to maximize the value of Michel electron hit purity (*83 %*) and hit completeness (*74 %*).*

A list of criteria has been used to select muon tracks and identify Michel electron candidates. details.

One of them proposed to determine the endpoint of a muon track, an the starting point of the Michel electron track, by searching for a sharp angle under $130°$ in the reconstructed track. While this method proved its effectiveness it exclude many potential Michel electron candidate which go in the same direction of the initial muon. This intership will invistigate an other method: looking at the energy deposit as a function of the track length of the muon. A cosmic muon has mostly a constant energy deposit $\mathrm{d}E/\mathrm{d}x$ of 2.1 MeV/cm in LAr but it diverges immediatly before the muon comes to rest and decay forming what is known as a Bragg peak (cf. Figure 5). The idea is to use this phenomenon to tag the endpoint of muon tracks and consider the continuation of the track beyond the Bragg peak as a candidate Michel electron track.

Space charge effect: Taking into account the shielding of drifting electrons and heavy ions on the local exterior electric field (on Ar inonization/scintillation ratio, and electron drifting trajectories/speed)

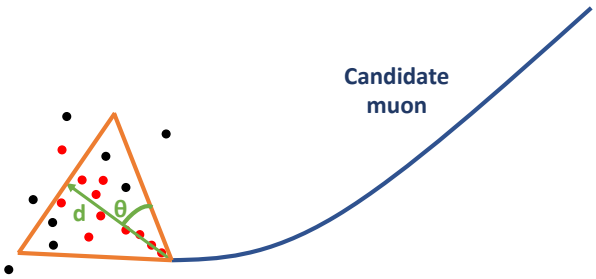

Figure 4: Red dots: true Michel electron hits , black dots: background events from nearby cosmic ray. All the hits contained inside the cone cuts are taken to be the candidate Michel electron hits [3].

4 Conclusion

neutrino interaction channels

neutrino sources and their energies

The maximal energy sensibility of the far detector is set to 2.6 GeV to maximize the $\nu_\mu \to \nu_e$ oscillation probability by adjusting the ratio E/L

Quenching: for the same $\mathrm{d}E/\mathrm{d}x$, two different particle deposit their energy through different channels.

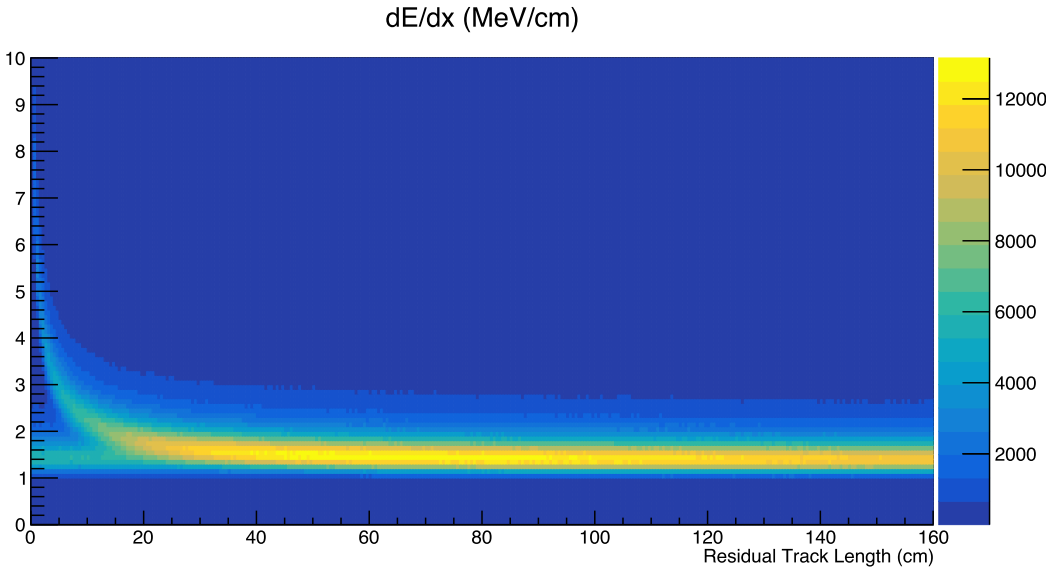

Figure 5: Energy deposit per distance of a muon with respect to the track lenght. Shortly before the endpoint of track, the energy deposit per distance diverges forming a Bragg peak. 10000-2800

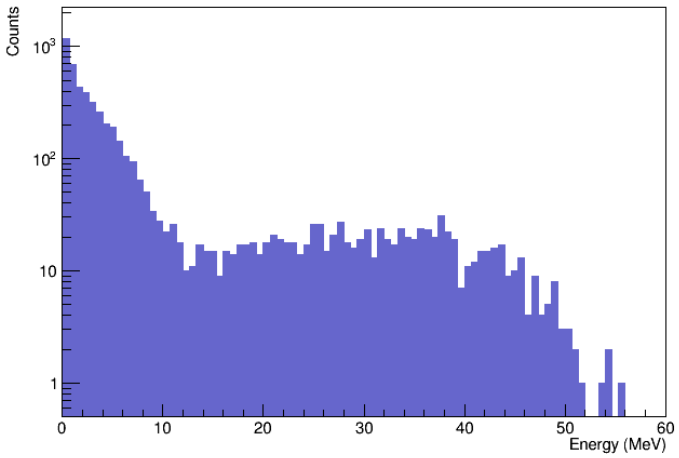

Figure 6: . 10000-2800

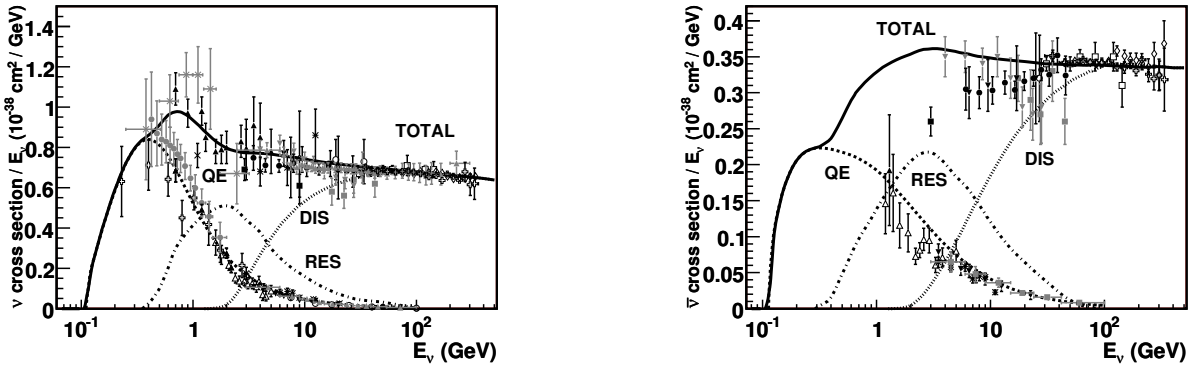

Figure 7: Total neutrino (left) and antineutrino (right) per nucleon charged current cross sections (for an isoscalar target) divided by neutrino energy and plotted as a function of energy. [4]

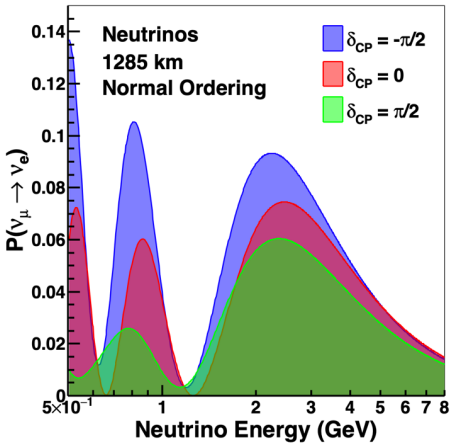

Figure 8: [1]

References

[1] B. Abi et al. "Long-baseline neutrino oscillation physics potential of the DUNE experiment: DUNE Collaboration". In: *The European Physical Journal C* 80.10 (Oct. 2020). ISSN: 1434-6052. DOI: 10.1140/epjc/s10052-020-08456-z. URL: http://dx.doi.org/10.1140/epjc/s10052-020-08456-z.

[2] S. Bilenky. *Neutrinos: Majorana or Dirac?* 2020. arXiv: 2008.02110 [hep-ph].

[3] DUNE Collaboration et al. *Identification and reconstruction of low-energy electrons in the ProtoDUNE-SP detector*. 2023. arXiv: 2211.01166 [hep-ex].

[4] J. A. Formaggio and G. P. Zeller. "From eV to EeV: Neutrino cross sections across energy scales". In: *Rev. Mod. Phys.* 84 (3 Sept. 2012), pp. 1307–1341. DOI: 10.1103/RevModPhys.84.1307. URL: https://link.aps.org/doi/10.1103/RevModPhys.84.1307.

[5] C. Giganti, S. Lavignac, and M. Zito. "Neutrino oscillations: The rise of the PMNS paradigm". In: *Progress in Particle and Nuclear Physics* 98 (2018), pp. 1–54. ISSN: 0146-6410. DOI: https://doi.org/10.1016/j.ppnp.2017.10.001. URL: https://www.sciencedirect.com/science/article/pii/S014664101730087X.

[6] S Al Kharusi et al. "SNEWS 2.0: a next-generation supernova early warning system for multi-messenger astronomy". In: *New Journal of Physics* 23.3 (Mar. 2021), p. 031201. DOI: 10.1088/1367-2630/abde33. URL: https://dx.doi.org/10.1088/1367-2630/abde33.